Design and Optimization of an Outer Rotor Spoke Type PMSM with Improved Saliency for a Lightweight Racing Vehicle

Hasan Can Karatepe
Dept. of Electrical & Electronics Engineering
Abdullah Gul University
Kayseri, TURKEY
hasancan.karatepe@agu.edu.tr

Burak Tekgun
Dept. of Electrical & Electronics Engineering
Abdullah Gul University
Kayseri, TURKEY
burak.tekgun@agu.edu.tr

Didem Tekgun
Dept. of Electrical & Electronics Engineering
Abdullah Gul University
Kayseri, TURKEY
didem.tekgun@agu.edu.tr

2024 7th International Conference on Electric Power and Energy Conversion Systems (EPECS) | 979-8-3315-1696-3/24/$31.00 ©2024 IEEE | DOI: 10.1109/EPECS62845.2024.10805520

***Abstract*— This paper presents the design and optimization of an outer rotor spoke-type permanent magnet synchronous motor, aimed at achieving high torque density. The improvement is accomplished by enhancing the saliency through a center shift of the rotor arc, while simultaneously minimizing cogging torque and torque ripple. The proposed design is optimized for an electro-mobile that will participate in TEKNOFEST's "Efficiency Challenge". A vehicle dynamics simulation with the parameters of the designed vehicle was done under the "New European Driving Cycle" (NEDC) to determine the required torque and speed values using MATLAB's "Virtual Vehicle Composer" application. The multi-objective differential evolution (MODE) algorithm was chosen for optimization and further altered for maximum torque per ampere (MTPA) angle sweep, since each optimization individual would have a different MTPA angle. The optimization was conducted with 40 generations and 522 individual designs. An optimal solution from the Pareto-Front was selected and its performance was investigated using the 2D finite element analysis (FEA).**

Keywords—PMSM, hub motor, spoke type IPM, MODE optimization, saliency.

I. INTRODUCTION

Permanent magnet (PM) machines have a wide range of applications with high power requirements. Such example is electric vehicles with ever-expanding topologies for efficient propulsion. PM machines are favorable for most electric vehicle applications with their torque and speed characteristics [1]. Over the years, PM machines have been rivaled against induction machines (IM) in the electric vehicle category. Most cases concluded that PMSMs outperform the IMs in efficiency manner on the same drive cycle and IMs were stated as needing to be optimized and improved to catch the power density and efficiency level of a PMSM [2], [3]. Various types of PMSMs with different magnet topologies are widely used for EV applications [4]. According to the torque and speed requirements of the application, both surface-mounted permanent magnet (SPM) and interior permanent magnet motors (IPMs) are preferred in the industry. While [5] indicated that an optimized SPM motor is suitable for a lightweight racing vehicle due to its high efficiency, comparisons in [6] and [4] demonstrate that spoke-type IPM motors significantly improve output torque and reduce cogging torque compared to similarly parameterized SPM motors. In case of overloading of the motor such as peak point in a drive cycle, IPM motors show superior results compared to an SPM motor [7]. Whilst [4] states a custom V-shaped PMSMs are efficient for an electric vehicle application, the cost of the magnets for a single pole is doubled compared to the spoke-type PMSM. The increased cost poses an obstacle, especially for budget-limited applications such as competitions. Therefore, outer rotor spoke type IPM motors as hub motor configuration on a lightweight racing vehicle would suit better with a similar optimization approach as [5].

While there are many rotor types for IPM motors, spoke-type IPM motor has many advantages primarily in the cost and manufacturing process, due to the simplicity of the rotor structure [8]. Researchers proposed that trapezoidal magnets can be utilized on spoke-type machines to prevent the slippage of the magnets and improve the output torque [6]. While trapezoidal magnets prevent slipping and improve the output torque, rare-earth materials with their frequently increasing cost are generally hard to find in distinct shapes such as trapezoidal, ultimately leading to higher cost of production. Using simple rectangular magnet blocks on the poles reduces the costs of machining magnets and those types of magnets are widely available [8]. Since the proposed machine is designed for an electric vehicle contest, cost consideration is a primary priority in the design process.

Another important omitted point in [5] is that cogging torque has a major impact on the launch of the vehicle. The cogging torque of the SPM machines is shown to be higher than the general IPM machines [4]. Many techniques were investigated over time for the reduction of the cogging torque. To a spoke-type machine, unequal airgap is one option for the purpose of cogging torque reduction [9]. By applying unequal airgap to the spoke type IPM, it can outperform an SPM machine in terms of cogging torque [6]. Moreover, slot and pole combination also has an impact on the cogging torque of brushless permanent magnet motors [10], so it is a design consideration on the proposed machine for minimizing its cogging torque.

In this paper, an outer rotor spoke type IPM machine that specialized for a contest called "Efficiency Challenge" is designed and optimized. A vehicle dynamics simulation for a lightweight vehicle is utilized according to the "New European Driving Cycle" (NEDC) driving cycle for observing the operation points of the motor. MATLAB's "Virtual Vehicle Composer" application is used as a simulation tool. Frequent operation points of the motor is determined and a single-point optimization for the most frequent torque and speed point is done with two optimization objectives; high torque density and efficiency. A similar MODE algorithm in [5] for single-point optimization with alterations for MTPA angle sweep is utilized in this paper. Sweeping the MTPA angle of each candidate design excessively increases the computational cost of the optimization, but it ensures the best possible performance of the candidate design. Analytical methods for the calculation of the MTPA angle as in [11] could decrease the computational cost of the optimization compared to the sweep method. However, the requirement of varying motor parameters makes integration difficult.

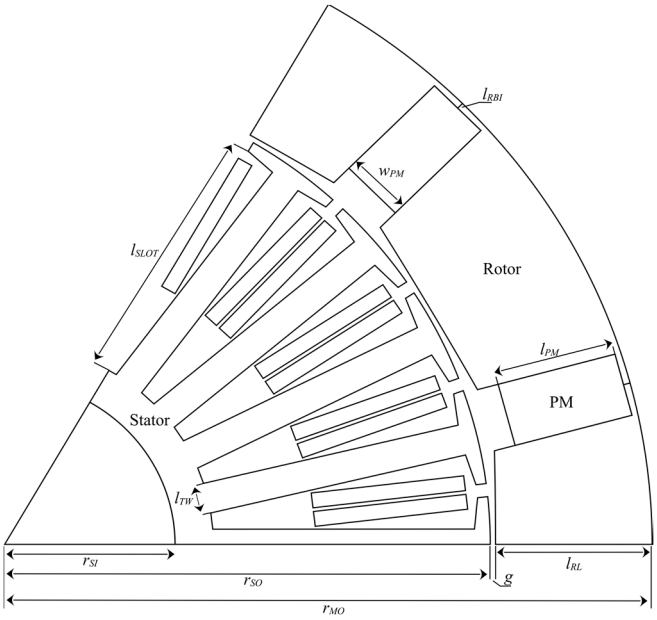

Fig. 1. 2D sketch of the motor with design parameters.

This paper is organized as follows: Section II gives details about the specifications and preliminary design considerations, and Section III describes the saliency improvement by the unequal airgap. Details of the vehicle dynamics simulation and its results are given in Section IV. Altered MODE optimization and the MTPA angle sweep are explained in Section V and the FEA results of the optimized machine are given in Section VI. The paper is concluded in Section VII.

II. Motor Specifications and Rotor Design

A. Desired Range of Specifications

As the aforementioned motor is designed for an electric vehicle that will participate in the "*Efficiency Challenge*" of the TEKNOFEST, there are several limitations on the design [12]. According to the limitations of the contest, the characteristics of the motor were adjusted and provided in Table I. As suggested in [10], the selected stator type in this study consists of double-layer windings to minimize the length of end turns in fractional-slot windings. The double-layer winding approach helps minimize the end winding lengths and copper losses, hence improving the efficiency of the overall machine. The size of the motor was determined by the tire size of the vehicle since the design is applied as a direct driving hub motor.

TABLE I. Predefined Characteristics of the Outer Rotor Spoke Type IPM Motor

Peak line voltage	210V
Rotor outer diameter	390mm
Stack length	40mm
Stator inner diameter	50mm
Stator slot opening	4mm
Material of magnets	NdFe35
Material of laminations	50JN270

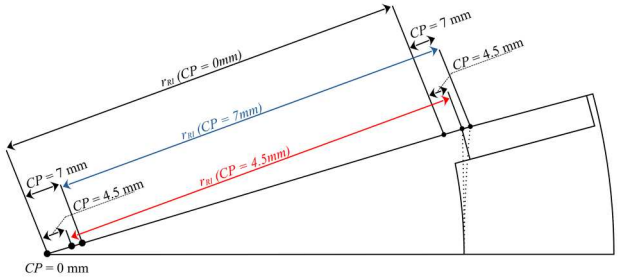

Fig. 2. Half pole of the motor with arc center position shift representation.

Due to the TEKNOFEST's limitation on the tire size is 90/90-16 [12], the outer diameter of the rotor cannot exceed 400 mm (approximately 16 inches) and the stack length should not exceed 50 mm. These limitations are influenced by the physical requirements for integrating the motor with the vehicle chassis and accommodating the motor housing that fits around the tires.

B. Selection of Slot and Pole Combination

It is crucial to keep the cogging torque minimal to ensure smooth propulsion of the vehicle. The slot and pole combination of the machine has a major impact on the cogging torque [10]. As stated in [10], there are combinations of the slot and pole numbers that provide smaller cogging torque. Moreover, integral-slot winding is usually unpreferred since it requires skewing, hence, fractional-slot winding combinations are used and performed for the proposed machine. Various slot and pole combinations are tested preliminary and the results are presented in Table II. 27 slot and 12 pole combination has the best cogging torque result among the others, hence, that model is selected and proceeded to the magnet dimension parameterization. Fig. 1 shows the design of the proposed machine.

TABLE II. Tested Slot and Pole Combinations For Cogging Torque

Number of slot and pole combinations	***Average cogging torque (Nm)***
30S/8P	1.4220
36S/8P	1.9042
42S/8P	1.8173
48S/8P	1.6285
30S/10P	1.5896
27S/12P	1.1610
45S/12P	1.7853

C. Determining the Magnet Dimensions

The rectangular magnets were parameterized in a way that magnet length is defined with the percentage of it in the rotor. This way, invalid geometries are avoided when the stator outer radius r_{SO} to motor outer radius r_{MO} ratio changes. The back iron of the rotor l_{RBI} is fixed at 2 mm to avoid the magnetic flux short-circuits on the magnet while retaining the structural integrity. Magnet width is noted by w_{PM} and defined in millimeters while the magnet depth is equal to the motor's stack length. As the chosen pole number is 12, the angle from the center of one magnet to the nearest magnet is calculated as 30 degrees.

III. Saliency Improvement With Rotor Pole Indent

The center position shift of the arc on the rotor's pole openings; *CP* is illustrated in Fig. 2 and used to generate unequal airgaps. This unequal airgap increases the saliency of the motor meanwhile reducing the cogging torque and torque ripple [6]. The length of the magnet is changing as the indent parameter differs. Also, torque ripple decreases with the optimal shift amount. Fig. 3 shows the cogging torque decreasing as the *CP* gets higher up to 5 mm. Besides, the back-EMF is seen to be decreasing too. Average output torque is decreasing whilst torque ripple is also decreasing as explained and shown in Fig. 4.

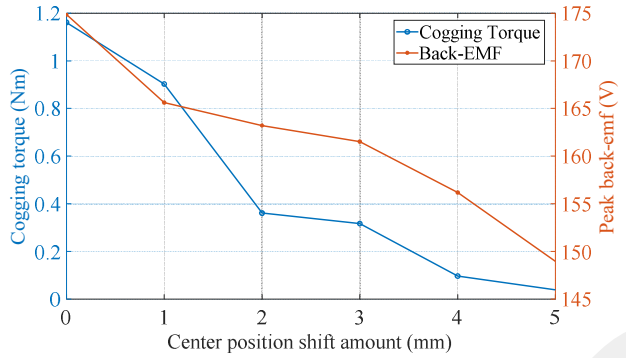

Fig. 3. Open circuit analysis with different CP values

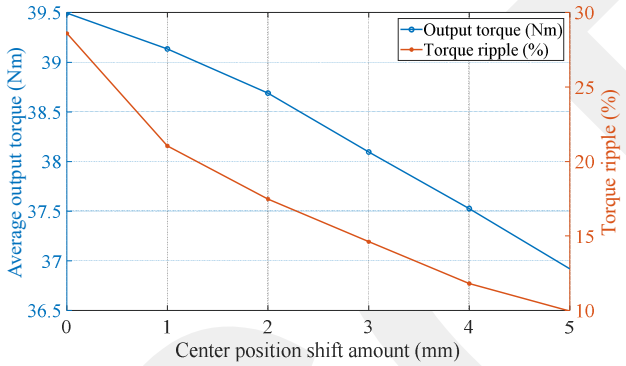

Fig. 4. On-load analysis with different *CP* values.

IV. Vehicle Dynamics Simulation

The maximum operation point of the machine has to be investigated before the optimization of the machine. Hence, a vehicle dynamics simulation is done for a lightweight race car with geometric parameters shown in Table III. These parameters are used on the MATLAB Virtual Vehicle Composer application and simulating the vehicle under NEDC leads to get the required torque and speed data versus the time of the motor. The details of the simulation are given in [13].

Although the Le Mans driving cycle would be a better candidate for the driving cycle simulation of a race car [14], the limitations of the motor driver and voltage limits of the Efficiency Challenge would not allow for this method. Since the track changes often in the Efficiency Challenge contest, it would be better to optimize the motor for NEDC to ensure the longevity of the design.

Here, the most frequent points in the torque and speed versus time data were investigated. By heatmap of the joint distribution of the torque and speed data, the most frequent points were observed. As shown in Fig. 5, the most frequent point of torque and speed values are 18.4748 Nm at 355.6859 rpm for one cycle of NEDC. While selecting these values for the optimization point would be suitable for the application, opting for slightly higher values with some headroom would provide resilience for the vehicle in different race tracks. Therefore, 400 rpm was selected as the base speed of the machine while it is expected to provide at least 25 Nm of torque.

TABLE III. Geometric Parameters of the Vehicle

Vehicle sprung mass	350 kg
Longitudinal distance from sprung mass to the front axle	1 m
Longitudinal distance from sprung mass to rear axle	1 m
Vertical distance from axle plane to sprung mass	0.12 m
Moment of inertia about the pitch axis	34.11 kg*m^2
The frontal area of the vehicle	1.77 m^2
Aerodynamic drag coefficient	0.33

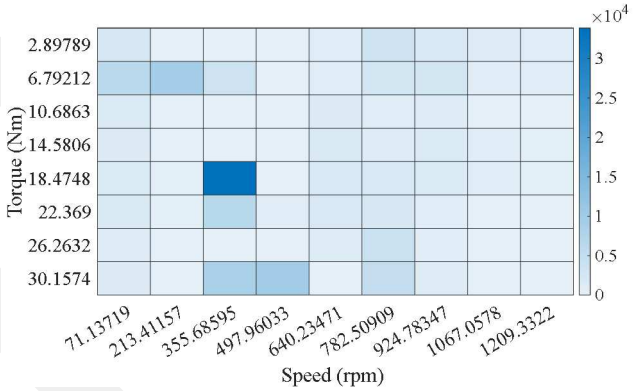

Fig. 5. Heatmap of the frequent torque and speed values.

V. Altered Differential Evolution Optimization

Multi-objective differential evolution algorithm was utilized for the optimization, with minor additions. As thoroughly detailed in [5], the MODE algorithm can be altered for various requirements as the flexibility and simplicity of the algorithm allow further modifications. The MODE algorithm illustrated in Fig. 6, works by iteratively improving a population of solutions. It starts by generating random solutions (parent vectors) representing potential designs. Each solution is analyzed using FEA to assess its performance. The algorithm can dynamically adjust the number of potential solutions it considers. If there's room for growth (PopS < MPS) and the optimization has progressed sufficiently (GenN > BPS), it creates additional solutions (mutant vectors) for exploration. New solutions (child vectors) are created by combining elements from existing solutions (parent and mutant vectors). These child solutions are then evaluated with FEA and compared to their parents. Only the superior solutions are chosen for the next generation. Promising solutions are added to a collection of top performers (Pareto front). A retraction algorithm that at specific intervals (GenN = multiple of PRV), the Pareto front is used to refine the parent vectors, potentially leading them towards even better designs. The process continues until a set number of generations (MaxGen) is reached. This iterative approach helps the

algorithm converge towards a set of optimal designs that balance different performance objectives. As this paper's

focus on the optimization stage is adding MTPA angle sweep to the already available altered MODE, details of this optimization method can be found in [5].

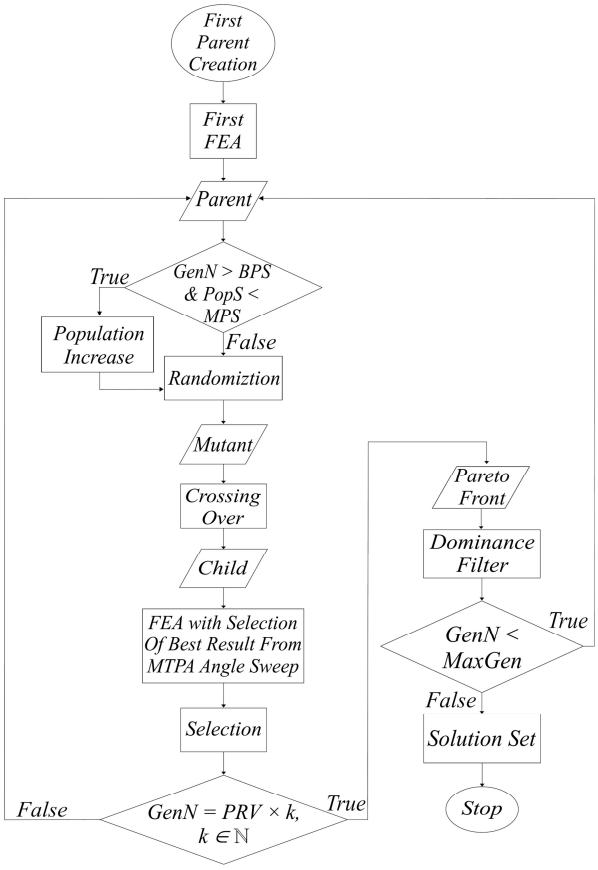

Fig. 6. Flowchart of MODE with MTPA angle sweep.

A. Altering MODE for MTPA Angle Sweep

In such a case of IPM motor optimization for maximum efficiency, maximum torque, or maximum torque density, the MTPA angle of the machine for each individual design has to be investigated. To achieve that, alterations were made to the algorithm explained above. For every individual in the population whether it was generated initially or it is a product of the genetic algorithm, a sweep of MTPA angle for it is done while in the FEA stage of the optimization. In the selection algorithm, the best-case scenario (highest average torque in such case) of the individual is selected and new solutions are created accordingly. The workflow of the altered MODE is shown in Fig. 6. This procedure ensures that the individual candidate can show its best under the MTPA control scheme, allowing the child vector to converge closer to the objective. Although this adjustment increases the computational effort required for the optimization, it ensures the results would represent the best possible cases for the design.

B. Objectives, Constraints, and Parameters of Optimization

a) Objectives: Unlike traditional races focused solely on speed, the Efficiency Challenge prioritizes achieving the most efficient vehicle. To reflect this focus, the optimization has two key objectives, which are increased torque density and efficiency. High torque density allows the motor to deliver more power in a compact size. In such a case with the fixed outer diameter, the stator and rotor's iron size affects the torque density. The average torque output could be an objective instead of torque density, however, as shown in Section III, the indent on the rotor has a negative effect on the average output torque. In fact, the optimizer would minimize the indent parameter "l_{INT}" and ignore its effect on cogging torque, torque ripple, and torque density. Overall, maximizing torque density and efficiency were the two most reasonable objectives for the optimization.

b) Constraints: As explained in [5], constraints are critical in such optimization in the case of an electric machine as the constraints prevent optimization from only prioritizing the objective without considering the boundaries that designs must stay within. The objectives define optimization to minimize or maximize the given output such as average output torque meanwhile the constraints limit the boundaries of other output parameters such as peak line voltage. As in this project, the Efficiency Challenge's so-called limitations on the peak line voltage is the main constraint, and the boundaries for it are given in Table IV.

TABLE IV. OPTIMIZATION CONSTRAINTS

Constraint	Calculation Method	Boundaries
Max. line voltage	$\max(V_{\Phi A} - V_{\Phi B}) + I_{rms} \times r_{copper}$	160 V – 200 V
Torque ripple	$\frac{Peak\ to\ peak\ torque}{Average\ torque} \times 100$	0 % – 20 %

Another constraint is the torque ripple; hence the magnet size is one major optimization parameter, and the magnet sizing has a major impact on the torque ripple while it also has an effect on the output torque. Besides, the sizable magnets tend to lead to higher output torque and torque density but also a higher torque ripple [6]. Higher torque ripple would cause the vehicle to not operate smoothly.

TABLE V. OPTIMIZATION PARAMETERS

Parameter	Definition	Boundaries
g [mm]	Airgap length	0.7 – 1.5
CP [mm]	Arc center position shift amount	0 – 5
k_{PM}	$\frac{l_{PM}}{l_{RL} - l_{RBI}}$	0.80 – 0.99
k_S	$\frac{r_{SO}}{r_{MO}}$	0.70 – 0.85
k_{SLOT}	$\frac{l_{SLOT}}{r_{SO} - r_{SI}}$	0.70 – 0.85
J [A/mm2]	Current density	1.5 – 4
I_{PEAK} [A]	Peak current	5 – 15
l_{TW} [mm]	Tooth width	7 – 14
w_{PM} [mm]	Magnet width	8 – 25

c) Parameters: This study relies heavily on using the MODE algorithm to optimize the motor's geometry, hence the geometry of the motor is parameterized on the Ansys Maxwell 2D in advance. As for the parameters of the optimization, the most significant ones that affect the objectives were selected. 9 parameters that were selected were shown in Table V with their boundaries respectively. Similar to [5], the number of turns for the winding was

expressed with the current, current density, and the area of the stator slot and it is defined in (1) where J is the current density, A_{slot} is the slot area and k_{fill} is the fill factor. The fill factor was selected as 0.25 as the higher amount would limit the manufacturing capability of the motor and the current density would exceed the limit of its boundary.

$$\#\ of\ Turns = \frac{J \times I_{rms}}{A_{slot} \times k_{fill}} \quad (1)$$

VI. 2-D FEA Results of the Proposed Motor

The optimization generates the Pareto Front data, the best candidate results in the whole population. The diamond-shaped variations that are seen in Fig. 7, are the results from the dominance filter. The best result from the filtered results was selected to be inspected on the FEA further. The parameters of the selected result are shown in Table VI. It is seen that the torque density and efficiency have an inverse relation, as the torque density gets high, the efficiency decreases and vice versa. The filtered results have approximately 10 Nm/m^3 of torque density difference between the maximum and minimum. The corresponding output torque of individual filtered results was observed and it was seen that the one with minimum torque density and maximum efficiency has a feasible amount of output torque in the operation point, and since efficiency is the priority in such a contest, the design with the highest efficiency and lowest cogging torque was selected. The selected result from the filter has the highest efficiency with 89.1259 % and 33.0846 Nm/m^3 of torque density. As already mentioned, the FEA was conducted on Ansys Maxwell 2D.

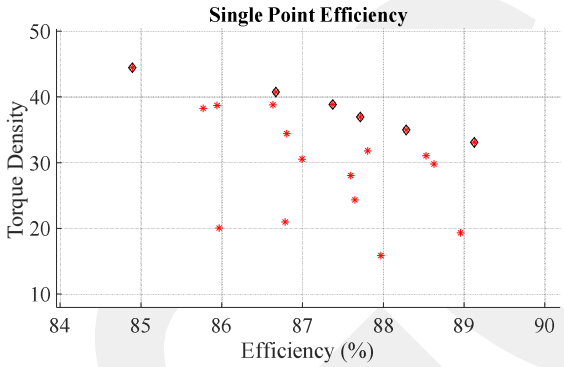

Fig. 7. Pareto Front of the optimization with dominance filter applied.

TABLE VI. Optimized Solution Parameters

Parameter	Boundaries
g [mm]	1.237905
l_{IND} [mm]	3.27992
k_{PM}	0.976365
k_S	0.8141914
k_{SLOT}	0.7775324
J [A/mm2]	2.419908
I_{PEAK} [A]	10.87448
l_{TW} [mm]	9.742222
w_{PM} [mm]	24.22798

A. No-Load FEA of the Motor

No-load FEA of the optimized motor was performed to observe the back-EMF and the cogging torque. The results are shown in Fig. 8 and Fig. 9, respectively. It is seen that the cogging torque is at acceptable levels with an average of 0.3530 Nm, ensuring the motor can rotate at such low speeds. Back-EMF includes minor harmonics and its phase-phase peak is at 168.3806 V.

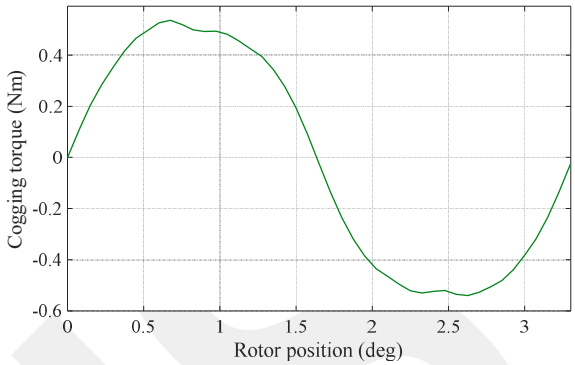

Fig. 8. Cogging torque variation obtained from FEA.

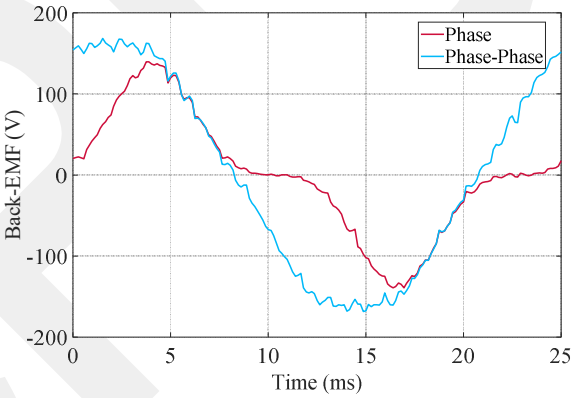

Fig. 9. Back-EMF waveform from FEA at 400 rpm.

B. Full-Load FEA of the Motor

Full-load FEA of the motor was conducted to observe the output torque and its ripple. The output torque at the rated current of 7.65 A_{rms} is shown in Fig. 10. Furthermore, the average output torque is 37.3856 Nm whilst the torque ripple is around 13.4281 %. These values are quite suitable for the aforementioned application. The efficiency map of the motor that is given in Fig. 11 shows that the motor operates at 85.3971 % efficiency at the most frequent point of the drive cycle.

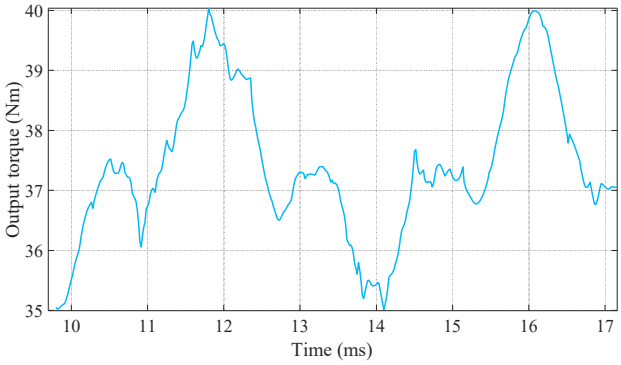

Fig. 10. Output torque at full load obtained from FEA

The efficiency map is obtained up until the field weakening region since the higher speeds are not necessary for such a contest application where the stability of the vehicle is more critical than its maximum speed. The highest efficiency of 92.066 % is obtained at the point of 700 rpm speed at 40.0682 Nm output torque.

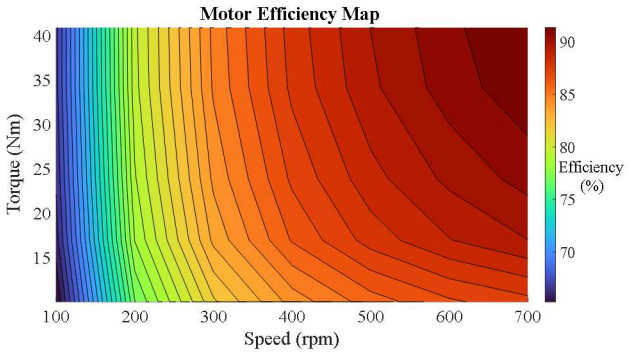

Fig. 11. Efficiency map of the optimized motor (up to 700 rpm)

VII. Conclusions

In this paper, an outer rotor spoke type IPM machine that specialized for a contest called "Efficiency Challenge" was designed and optimized. The best slot and pole combination variation is selected according to the minimal cogging torque. A vehicle dynamics simulation was done for a lightweight vehicle for the determination of the base speed and required torque output under the new European drive cycle (NEDC). To improve the saliency of the machine, a center position shift on the rotor pole arcs was added and the effects were observed. It was seen that the cogging torque of the machine was significantly improved with the shifted center position of the rotor pole arc. The motor is optimized with the altered MODE optimization method with an additional MTPA angle sweep step for each design. After 40 generations and 522 individual designs from the optimization, the optimized solution is further investigated in FEA. No-load FEA of the machine revealed that cogging torque is at the desired levels. The efficiency map of the motor (up to 700 rpm and 40 Nm) shows that the motor has 85.3971 % efficiency on the selected drive cycle point while the maximum efficiency can go up to 92.066 %. Compared to an SPM machine with a similar optimization topology, it is shown that higher torque density can be achievable with a spoke-type IPM machine. For future studies, manufacturing and lab tests of the motor will be conducted after performing the thermal and mechanical analyses of the motor.

References

[1] N. Grilo, D. M. Sousa and A. Roque, "AC motors for application in a commercial electric vehicle: Designing aspects," *2012 16th IEEE Mediterranean Electrotechnical Conference*, Yasmine Hammamet, Tunisia, 2012, pp. 277-280, doi: 10.1109/MELCON.2012.6196432.

[2] V. T. Buyukdegirmenci, A. M. Bazzi and P. T. Krein, "Evaluation of Induction and Permanent-Magnet Synchronous Machines Using Drive-Cycle Energy and Loss Minimization in Traction Applications," in *IEEE Transactions on Industry Applications*, vol. 50, no. 1, pp. 395-403, Jan.-Feb. 2014, doi: 10.1109/TIA.2013.2266352.

[3] J. P. Trovao, P. G. Pereirinha and F. J. T. E. Ferreira, "Comparative study of different electric machines in the powertrain of a small electric vehicle," *2008 18th International Conference on Electrical Machines*, Vilamoura, Portugal, 2008, pp. 1-6, doi: 10.1109/ICELMACH.2008.4800164.

[4] N. Murali, S. Ushakumari and M. V. P, "Performance comparison between different rotor configurations of PMSM for EV application," *2020 IEEE REGION 10 CONFERENCE (TENCON)*, Osaka, Japan, 2020, pp. 1334-1339, doi: 10.1109/TENCON50793.2020.9293844.

[5] M. M. Cosdu, A. F. Hacan and B. Tekgun, "Design Optimization of an Outer Rotor PMSM for a Drive Cycle using an Improved MODE Algorithm for a Lightweight Racing Vehicle," *2020 6th International Conference on Electric Power and Energy Conversion Systems (EPECS)*, Istanbul, Turkey, 2020, pp. 58-63, doi: 10.1109/EPECS48981.2020.9304956.

[6] K. Xie, D. Li, R. Qu and D. Jiang, "Analysis and experimental comparison of spoke type and surface mounted PM machines with fractional slot concentrated winding," *2016 19th International Conference on Electrical Machines and Systems (ICEMS)*, Chiba, Japan, 2016, pp. 1-6.

[7] A. Vagati, G. Pellegrino and P. Guglielmi, "Comparison between SPM and IPM motor drives for EV application," *The XIX International Conference on Electrical Machines - ICEM 2010*, Rome, Italy, 2010, pp. 1-6, doi: 10.1109/ICELMACH.2010.5607911.

[8] Y. Demir and M. Aydin, "Design of a spoke type IPM synchronous motor with segmented rotor for low DC voltage applications," *2014 IEEE Energy Conversion Congress and Exposition (ECCE)*, Pittsburgh, PA, USA, 2014, pp. 3556-3561, doi: 10.1109/ECCE.2014.6953884.

[9] N. Bianchi and S. Bolognani, "Design techniques for reducing the cogging torque in surface-mounted PM motors," in *IEEE Transactions on Industry Applications*, vol. 38, no. 5, pp. 1259-1265, Sept.-Oct. 2002, doi: 10.1109/TIA.2002.802989.

[10] J. R. Hendershot and T. Miller, "Design of brushless Permanent-Magnet motors," in *Oxford University Press eBooks*, 1995. doi: 10.1093/oso/9780198593898.001.0001.

[11] P. Zhang, "A novel design optimization of a fault-tolerant AC permanent magnet machine-drive system," Ph.D. dissertation, Elect. Comput. Eng. Dept., Marquette Univ., Milwaukee, WI, USA, Dec. 2013.

[12] Scientific and Technological Research Council of Turkey (TÜBİTAK), "International Efficiency Challenge Electric Vehicle 2024 Rules," https://cdn.teknofest.org/media/upload/userFormUpload/International_EC_Domestic_Product_Rules_2024_ENG_Y1.V1.8_UB0f9.pdf, 2024.

[13] Mathworks, "Configure, build, and analyze a virtual automotive vehicle," https://www.mathworks.com/help/vdynblks/ref/virtualvehiclecomposer-app.html, (accessed Jul. 5, 2024).

[14] A. Fatemi, D. M. Ionel, M. Popescu, Y. C. Chong and N. A. O. Demerdash, "Design Optimization of a High Torque Density Spoke-Type PM Motor for a Formula E Race Drive Cycle," in *IEEE Transactions on Industry Applications*, vol. 54, no. 5, pp. 4343-4354, Sept.-Oct. 2018, doi: 10.1109/TIA.2018.2844804.